

## On the number of principal components in high dimensions

BY SUNGKYU JUNG

*Department of Statistics, University of Pittsburgh, Pittsburgh, Pennsylvania, 15260, U.S.A.*

sungkyu@pitt.edu

MYUNG HEE LEE

*Center for Global Health, Department of Medicine, Weill Cornell Medicine, New York, New*

*York, 10065, U.S.A.*

myl2003@med.cornell.edu

AND JEONGYOUN AHN

*Department of Statistics, University of Georgia, Athens, Georgia, 30602, U.S.A.*

jyahn@uga.edu

### SUMMARY

We consider the problem of how many components to retain in the application of principal component analysis when the dimension is much higher than the number of observations. To estimate the number of components, we propose to sequentially test skewness of the squared lengths of residual scores that are obtained by removing leading principal components. The residual lengths are asymptotically left-skewed if all principal components with diverging variances are removed, and right-skewed if not. The proposed estimator is shown to be consistent, performs

well in high-dimensional simulation studies, and provides reasonable estimates in a number of real data examples.

*Some key words:* High dimension low sample size; Pervasive factor; Principal component analysis; Principal component score; Skewness test.

## 1. INTRODUCTION

Principal component analysis is widely used in multivariate analysis, and has shown to be effective in dimension reduction of modern high-dimensional data. Let  $\mathcal{X} = [X_1, \dots, X_n]^T$  be an  $n \times d$  data matrix, where each column vector has zero mean and covariance matrix  $\Sigma_d = \sum_{i=1}^d \lambda_i u_i u_i^T$ , and  $(u_i, \lambda_i)$  denotes the  $i$ th principal component direction and variance. The classical estimates  $(\hat{u}_i, \hat{\lambda}_i)$  are obtained by the eigen-decomposition of the sample covariance matrix. Determining the number of components to retain is a crucial problem in applications of principal component analysis.

A number of strategies have been proposed to tackle this problem in the conventional data situation, where the sample size is large and the dimension is relatively low, i.e.,  $d \ll n$ . These include the graphical methods based on the scree plot of eigenvalues, model-based tests, and computer-intensive tools (Jolliffe, 2002; Josse & Husson, 2012). However, modern data challenges often involve the high dimension, low sample size data situation, i.e.,  $d \gg n$ . Under such situations, those methods may be infeasible, computationally prohibitive, or based on subjective choice. In this article, we propose a novel estimator of the number of components, specifically designed for the  $d \gg n$  case.

The true number of components is defined in terms of eigenvalues  $\lambda_i$  of  $\Sigma_d$ . A popular approach is to assume that the first  $m$  eigenvalues are larger than a threshold, say  $\tau^2$ , and the rest of eigenvalues are equal to  $\tau^2$ . This spike model (Johnstone, 2001; Paul, 2007) has been used in

many different contexts (Baik & Silverstein, 2006; Kritchman & Nadler, 2009; Leek, 2011). For diverging dimension  $d$  with limited sample size, it has been known that the size of ‘spike’ should be increasing at least at the same order as  $d$  in order to have a non-trivial eigenvector estimates (Lee, 2012). Consequently, we assume the eigenvalues of  $\Sigma_d$  to be

$$\lambda_i = \sigma_i^2 d \quad (i = 1, \dots, m), \quad \sigma_1^2 > \dots > \sigma_m^2 > 0, \quad (1)$$

and the rest of eigenvalues  $\{\lambda_{m+1}, \dots, \lambda_d\}$  to be equal to each other or form a slowly-decreasing sequence. Our model is indeed general, and is defined in Section 3.

Hellton & Thoresen (2017) has shown that under the  $m$ -component models of (1), even though the classical estimates of  $(\lambda_i, u_i)$  are inconsistent for increasing dimension, the first  $m$  estimated principal component scores contain useful information on the true scores. We further show in Section 5 that the rest of estimated scores are mostly accumulated noises, which implies that the number of spikes  $m$  in (1) can be considered as the number of asymptotically meaningful components.

To determine  $m$  from a given sample  $\mathcal{X}$ , we propose to sequentially test the null hypothesis  $H_k : m = k$  against the alternative hypothesis  $H_{a,k} : m > k$ , for increasing values of  $k$ , and to estimate  $m$  by the smallest  $k$  for which  $H_k$  is not rejected. To this aim, we show that the squared lengths of residuals that are obtained by removing the first  $k$  leading principal components are asymptotically left-skewed under the null hypothesis, or right-skewed under the alternative hypothesis. This observation motivates us to consider test statistics based on the empirical distribution of the residual lengths. We adopt well-known tests for skewness (Randles et al., 1980; D’Agostino & Pearson, 1973). The resulting estimator is consistent under a mild condition.

We demonstrate our approach in both simulated and real data sets, including high-dimensional gene expression and image data. In comparison to a number of existing methods, summarized

in Section 4.1, our method provides reasonable estimates. We conclude with a discussion on the effectiveness of estimated principal components.

## 2. SEQUENTIAL TESTS TO DETERMINE $m$

### 2.1. Motivation

We propose to sequentially test the set of null hypotheses  $\{H_0, H_1, \dots, H_M\}$  for some  $M < n$ , against one-sided alternatives:

$$H_k : m = k \quad \text{vs.} \quad H_{a,k} : m > k, \quad (2)$$

where  $m$  is the number of components with fast-diverging variances in (1). These null hypotheses do not overlap; if  $H_k$  is true, then  $H_\ell$  is not true for all  $\ell \neq k$ . However,  $H_k$  is nested within all lower-order alternatives; if  $H_k$  is true, then  $H_{a,\ell}$  is true for all  $\ell < k$ . These observations suggest to test  $H_k$  only if  $H_\ell$  is rejected for all  $\ell < k$ . The number of effective components,  $m$ , is then determined by the smallest  $k$  for which  $H_k$  is not rejected at a given level.

To test these hypotheses, we first note that the squared lengths of data vectors  $\|X_j\|_2^2$  ( $j = 1, \dots, n$ ) have different empirical distributions depending on which, null or alternative, hypothesis is true. As an illustrative example, let us first assume that the global null  $H_0$  is true, specifically,  $\Sigma_d = \tau^2 I_d$ . It can be shown that the squared length  $\|X_j\|_2^2$  is normally distributed for large  $d$ :

$$\sqrt{d} \left( d^{-1} \|X_j\|_2^2 - \tau^2 \right) \sim N(0, 2\tau^4). \quad (3)$$

On the other hand, when  $m \geq 1$  in (1), it is easy to see that the squared length is decomposed into a sum of two independent random variables: Assuming  $m = 1$  and the data are normal,  $d^{-1} \|X_j\|_2^2 = Z + Y$ , where the distributions of  $Z$  and  $Y$  are approximately

$$Z \sim N(\tau^2, 2\tau^4/d), \quad Y/\sigma_1^2 \sim \chi_1^2. \quad (4)$$

In the limit  $d \rightarrow \infty$ ,  $Z$  degenerates to  $\tau^2$ , thus  $d^{-1} \|X_j\|_2^2$  converges in distribution to a shifted-and-scaled chi-square random variable, which is right-skewed.

The above example suggests to consider test statistics based on the normality or the skewness of the empirical distribution of the squared lengths. We will show in Section 3 that general asymptotic null and alternative distributions of the squared lengths are similar to those in (3) and (4), even under a non-Gaussian assumption.

### 2.2. Test statistics

In testing the global null hypothesis, the asymptotic normality, shown in (3) under  $H_0$ , can be used. Let  $p_0^N = p^N(\|X_1\|_2^2, \dots, \|X_n\|_2^2)$  be a p-value in testing the normality of  $\|X_j\|_2^2$ . Intuitively, if a principal component with large variance is present,  $p_0^N$  tends to be small, since the empirical distribution becomes right-skewed as shown in (4).

For testing higher-order hypotheses  $H_k$  for  $k \geq 1$ , we propose to remove the first  $k$  estimated principal components from the data. We use the classical estimates  $(\hat{u}_i, \hat{\lambda}_i)$  of the principal component direction vector and variance pair  $(u_i, \lambda_i)$  ( $i = 1, \dots, n$ ) obtained by the eigen-decomposition of the sample covariance matrix  $S_d = n^{-1} \mathcal{X}^T \mathcal{X} = \hat{U} \hat{\Lambda} \hat{U}^T$ . Denote the scaled squared length of the  $k$ th residual for the  $j$ th observation by

$$R_j(k) = \frac{1}{d} \left\| X_j - \sum_{i=1}^k \hat{u}_i \hat{u}_i^T X_j \right\|_2^2, \quad (j = 1, \dots, n; k = 0, \dots, M). \quad (5)$$

The normality test may be adopted in computing p-values for testing  $H_k$ . We will show later in Section 3.2 that if  $\hat{u}_i$  were a consistent estimator of  $u_i$  in the  $d$ -limit for  $i \leq k$ , then the asymptotic null distribution of  $R_j(k)$  is Gaussian under  $H_k$ , thus leading to a uniform null distribution of the p-value.

There are, however, limited situations where  $\hat{u}_i$  would be consistent for the growing dimension. In fact, under the fast-diverging eigenvalue assumption (1) and in the high dimension, low

sample size asymptotic scenario, the first  $m$  sample principal component directions are *inconsistent*, while the rest are *strongly inconsistent* with their population counterparts (Jung et al., 2012b; Lee, 2012). Moreover, the true principal component variance  $\lambda_i$  is often over-estimated by  $\hat{\lambda}_i$  for  $i \leq m$ . Since the sum of squared scores equals the variance, i.e.,  $n^{-1} \sum_{j=1}^n (\hat{u}_i^T X_j)^2 = \hat{\lambda}_i$ , this overestimation affects (5) in such a way that  $R_j(k)$  becomes smaller than desired. Thus the empirical distribution of  $R_j(k)$  is stochastically smaller than the said asymptotic normal distribution, and becomes left-skewed (or left-tailed). We will revisit this phenomenon in Section 3.3.

To incorporate the left-skewed  $R_j(k)$ , our first choice of the test statistic is from a test for skewness. For observations  $y_j = R_j(k)$  ( $j = 1, \dots, n$ ), suppose the distribution of  $y_j$  is continuous with unknown median  $\theta$ . Randles et al. (1980) proposed a nonparametric test for symmetry about  $\theta$  based on a  $U$ -statistic with kernel

$$f^*(y_i, y_j, y_k) = \text{sign}(y_i + y_j - 2y_k) + \text{sign}(y_i + y_k - 2y_j) + \text{sign}(y_j + y_k - 2y_i).$$

This test is sometimes called triples test for symmetry. The triples test is an asymptotic test for large  $n$ , and Randles et al. (1980) recommended to use its asymptotic normality when  $n > 20$ . A one-sided test for left- or right-skewed alternatives is also possible (Hollander et al., 2013, Section 3.9). For our purpose, the p-value is obtained by the asymptotic normality for one-sided triples test with the alternative of right-skewed distributions, and is denoted by

$$p_k^R = p^R\{R_1(k), \dots, R_n(k)\}. \quad (6)$$

Our second choice of the test statistic is obtained from a test for normality that is specially designed to be sensitive toward skewed alternatives. This test is based on the sample skewness coefficient  $b_1 = m_3/(m_2)^{3/2}$ , where  $m_r = n^{-1} \sum_{j=1}^n (y_j - \bar{y})^r$ . D'Agostino (1970) suggested a transformation of  $b_1$ , defining  $Z = \delta \log[b_1/\lambda + \{(b_1/\lambda)^2 + 1\}^{1/2}]$ , where  $\delta$  and  $\lambda$  are functions of the theoretical moments of  $b_1$  in samples from the normal distribution, and in turn are simply

functions of the sample size  $n$ . The distribution of the transformed  $Z$ , under normal assumptions, is well-approximated by the standard normal, even for a small sample size  $n \geq 8$  (D'Agostino, 1970; D'Agostino & Pearson, 1973). Positive  $b_1$  and  $Z$  indicate right-skewness, while their negative values indicate left-skewness. For  $H_k$  ( $k = 0, \dots, M$ ), the p-value of the skewness test is defined by

$$p_k^D = p^D\{R_1(k), \dots, R_n(k)\} = 1 - \Phi(Z), \quad (7)$$

where  $\Phi$  is the distribution function of the standard normal.

Both p-values in (6)-(7) have the uniform distribution if the null distribution of  $R_j(k)$  is normal. The p-values are sensitive to the right-skewed alternatives, as they tend to be close to zero under such cases. On the other hand, if the null distribution of  $R_j(k)$  is left-skewed, the p-values are close to 1. Other tests of symmetry (*cf.* Farrell & Rogers-Stewart, 2006) can be used in place of (6)-(7).

### 2.3. Example

Before proceeding with theoretical results, we demonstrate the proposed test procedures on a real data set from a microarray study. This data set, described in detail in Bhattacharjee et al. (2001), contains  $d = 2530$  genes from  $n = 56$  patients in four different lung cancer subtypes. An inspection of principal component scores plot (see, e.g., Fig. 1 in Jung & Marron (2009)) suggests that the four subtypes are visually separated by using the first few sample principal components, and there is no outlier in the data. It has been believed that the sample principal component analysis provides a reasonable dimension reduction, but there has been no attempt to systematically determine the number of effective components for this dataset.

We applied the tests discussed in Section 2.2 to obtain sequences of p-values in testing (2). As a visual tool to determine the number of components, we plot  $p_k^R$  and  $p_k^D$  against  $k$ , as shown

in the top left panel of Fig. 1. Graphical methods based on the scree plot, shown in the top right panel of Fig. 1, lead to either  $\hat{m} = 2$  when locating an ‘elbow,’ or  $\hat{m} = 17$  when using a heuristic cutoff based on the cumulative percentage of variance explained, say 80%. In contrast, our estimate, using either of the two test statistics, is  $\hat{m} = 9$ , based on

$$\hat{m} = \min\{k : p_k > \alpha\}, \quad (8)$$

where  $\alpha = 0.1$ , in this example.

The empirical distribution of  $R_j(0)$  in the bottom left panel of Fig. 1 is clearly right-skewed, which shows a strong evidence against  $H_0 : m = 0$ . The components with large variances contained in  $R_j(0) = d^{-1} \|X_j\|^2$  yield the heavy-tailed distribution skewed to large values. On the other hand, noise-accumulated components are excessively taken out from  $R_j(15)$ , leading to the left-skewed distribution of residual lengths, as shown in the bottom right panel. In this example, p-values in the sequences are small for the first few, then show a sharp transition to high values close to 1. This pattern of p-value sequence was also found in many real and simulated data sets, and seems to be typical.

### 3. ASYMPTOTIC NULL AND ALTERNATIVE DISTRIBUTIONS

#### 3.1. Models

We model that the variances of the first  $m$  components are fast-diverging at the rate of  $d$ , while the rest are assumed to be much smaller. It seems standard to assume  $m$  is fixed as the variances are diverging. For a fixed  $m$ , the  $m$ -component model is defined for increasing  $d$  in Conditions 1–4 below.

*Condition 1.*  $\lambda_i = \sigma_i^2 d$  ( $i = 1, \dots, m$ ),  $\sigma_1^2 > \dots > \sigma_m^2 > 0$ .

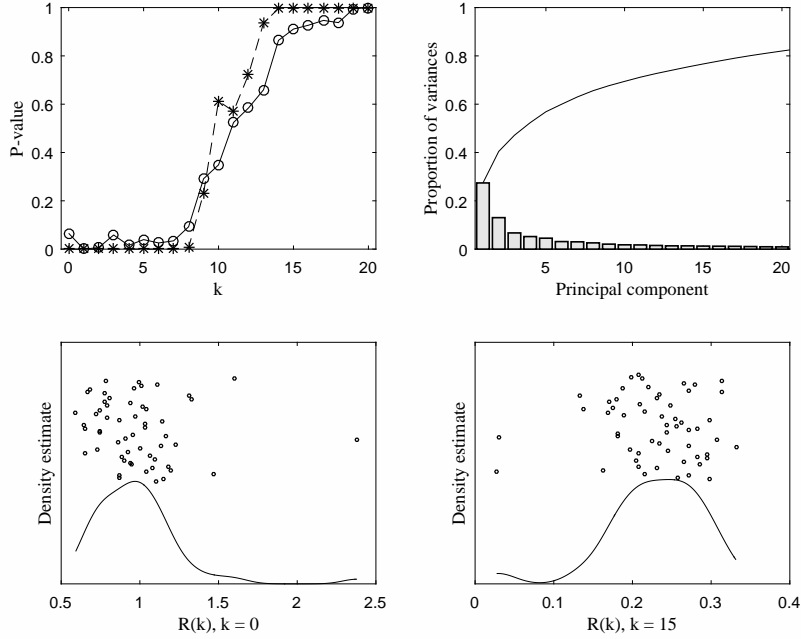


Fig. 1. Top left: sequences of p-values computed from a microarray data set (Bhattacharjee et al., 2001);  $p_k^R$  (circle-solid) and  $p_k^D$  (asterisk-dashed). Top right: scree plot. Bottom panels: empirical distributions of  $R_j(0)$  and  $R_j(15)$  by a kernel density estimate and a jitterplot.

*Condition 2.*  $\sum_{i=m+1}^d \lambda_i/d \rightarrow \tau^2 \in (0, \infty)$ ,  $\sum_{i=m+1}^d \lambda_i^2/d \rightarrow v_O^2 \in (0, \infty)$  as  $d \rightarrow \infty$ , and there exists  $\delta \in (0, 1]$  such that  $\sum_{i=m+1}^d \lambda_i^{2+\delta} = o(d^{1+\delta/2})$ .

By decomposing each observation into the first  $m$  principal components and the remaining term, we write  $X_j = \sum_{i=1}^m \lambda_i^{1/2} u_i z_{ij} + \sum_{i=m+1}^d \lambda_i^{1/2} u_i z_{ij}$  ( $j = 1, \dots, n$ ), where  $z_{ij}$  is the normalized principal component score.

*Condition 3.* For each  $j = 1, 2, \dots$ ,  $Z_j = (z_{1j}, z_{2j}, \dots)$  is a sequence of independent random variables such that for any  $i$ ,  $E(z_{ij}) = 0$ ,  $\text{var}(z_{ij}) = 1$ , and that the second and third moments of  $z_{ij}^2$  are uniformly bounded below and above. For  $j \neq \ell$ ,  $Z_j$  and  $Z_\ell$  are independent.

Conditions 1 and 2 are quite general and encompass the spike models of Leek (2011) and Hellton & Thoresen (2017). In particular, they include equal ( $\lambda_{m+1} = \dots = \lambda_d$ ), polynomially-

decreasing ( $\lambda_i = i^{-\beta}$  for  $0 \leq \beta < 0.5$ ), and slowly-diverging eigenvalues ( $\lambda_{m+1} = \cdots = \lambda_{m+\nu} = d^\gamma$  and  $\lambda_{\nu+1} = \cdots = \lambda_d = \tau^2$ , where  $\nu \asymp d^\beta$ , and  $2\gamma + \beta < 1$ ). It is worth noting that Condition 2 is stronger than the conditions of Ahn et al. (2007), which are used in showing the high-dimension, low-sample-size geometric representation: Modulo rotation, the data converge to a regular simplex (Hall et al., 2005). This stronger condition and the moment conditions in Condition 3 are needed in introducing a  $d$ -asymptotic normality in Theorem 1 and also in describing asymptotic behaviors of sample scores in Theorem 4. We note that Conditions 1 and 2 imply a low “effective rank” assumption in the random matrix literature; see Koltchinskii et al. (2016, 2017) for relevant results.

A special case of our model is the high-dimensional approximate factor model with pervasive factors, defined below, which has recently gained popularity as it is believed to be more realistic than other models (Hellton & Thoresen, 2017). Let  $X = \sum_{i=1}^m q_i z_i + \epsilon$  be an  $m$ -factor model, where  $z_i$  ( $i = 1, \dots, m$ ) are standardized factor scores,  $\epsilon = (\epsilon_1, \dots, \epsilon_d)^\top$  is a mean-zero independent noise vector with uniformly bounded variances. The orthogonal factor loadings,  $q_i \in \mathbb{R}^d$ , are pervasive, that is, the proportion of non-zero entries of  $q_i$  is non-vanishing as  $d$  increases (Fan et al., 2013; Hellton & Thoresen, 2017). For example,  $q_i$  is pervasive if for  $r \in (0, 1)$  the first  $\lfloor rd \rfloor$  entries of  $q_i$  are one, while the rest  $d - \lfloor rd \rfloor$  entries are zero for all  $d$ . The loading vector  $q_i$  is then expressed as  $q_i = \lambda_i^{1/2} u_i$ , where  $\|u_i\|_2 = 1$  and  $\lim_{d \rightarrow \infty} \lambda_i/d = \sigma_i^2$ . Condition 1 makes the first  $m$  components pervasive. Intuitively, when more variables are added into the analysis (i.e., the dimension  $d$  increases), these added variables are not simply noises but are correlated with the pervasive factors.

The following assumption on the pervasive factors plays a crucial role in our test procedures proposed in Section 2.2.

*Condition 4.* The third central moment of  $z_{ij}^2$  ( $i = 1, \dots, m, j = 1, \dots, n$ ) is positive.

Simply put, we require that  $z_{ij}^2$  is *right-skewed*. We believe Condition 4, which is a relaxation from Gaussian assumption, is quite general. It holds for many known distributions, including  $t$ -distributions with degrees of freedom  $\nu > 6$ , the beta distributions with parameters  $(\alpha, \alpha)$  with  $\alpha > 0.5$ , the gamma distributions, and a normal mixture  $\xi X_1 + (1 - \xi)X_2$ , where  $X_1$  and  $X_2$  are independent normal random variables with a common variance, and  $\xi$  follows a Bernoulli distribution.

### 3.2. The case of known principal component directions

We first investigate an ideal case where the principal component directions are known, to better understand the high-dimensional asymptotic behavior of the residual lengths. Define the  $k$ th *true* residual length of the  $j$ th observation by

$$\tilde{R}_j(k) = d^{-1} \left\| X_j - \sum_{i=1}^k u_i u_i^T X_j \right\|_2^2 = d^{-1} \sum_{i=k+1}^d w_{ij}^2, \quad (9)$$

where  $w_{ij} = u_i^T X_j = \lambda_i^{1/2} z_{ij}$  is the population principal component score.

The asymptotic behaviour of (9) can be understood by using a scaled Gram matrix  $S_D = d^{-1} \mathcal{X} \mathcal{X}^T$ , whose  $(j, k)$ th element is  $s_{jk} = d^{-1} X_j^T X_k$ ,  $1 \leq j, k \leq n$ . An immediate connection is that the  $j$ th diagonal element of  $S_D$  is  $\tilde{R}_j(0)$ . Under the assumption of  $m$  fast-diverging components, we denote the  $n \times m$  matrix of the first  $m$  scaled components by  $W_1^T = d^{-1/2} \mathcal{X}(u_1, \dots, u_m)$ , where the  $(i, j)$ th element of  $W_1$  is  $d^{-1/2} w_{ij}$ . It is known that  $S_D$  has a limiting expression (Jung et al., 2012b);

$$S_D \rightarrow W_1^T W_1 + \tau^2 I_n, \quad d \rightarrow \infty, \quad (10)$$

in probability, conditional on  $W_1$ . This result is now strengthened to provide a rate of convergence of  $S_D$ .

THEOREM 1. Assume the  $m$ -factor model under Conditions 1–3. Let  $m \geq 0$  be fixed. Conditioned on the pervasive factors  $W_1$ , (10) holds. Moreover, each element of  $S_D$  has a  $d$ -asymptotic normal distribution: As  $d \rightarrow \infty$ ,

$$\begin{aligned} \sqrt{d} \left( s_{jj} - \sum_{i=1}^m \sigma_i^2 z_{ij}^2 - \tau^2 \right) &\longrightarrow N(0, v_D^2) \quad (j = 1, \dots, n), \\ \sqrt{d} \left( s_{jk} - \sum_{i=1}^m \sigma_i^2 z_{ij} z_{ik} \right) &\longrightarrow N(0, v_O^2) \quad (j, k = 1, \dots, n; j \neq k) \end{aligned}$$

in distribution, where  $v_D^2 = \lim_{d \rightarrow \infty} \sum_{i=m+1}^d \lambda_i^2 \text{var}(z_{ij}^2)/d$  and  $v_O^2 = \lim_{d \rightarrow \infty} \sum_{i=m+1}^d \lambda_i^2/d$ .

The asymptotic normality in Theorem 1 provides the null and alternative distributions of  $\tilde{R}_j(k)$ .

COROLLARY 1. Assume the  $m$ -factor model under Conditions 1–4. Let  $n > m \geq 0$  be fixed. Then for any  $j = 1, \dots, n$  and  $k = 0, 1, \dots, n-1$ , for large  $d$ ,

- (i) if  $k \geq m$ ,  $\tilde{R}_j(k)$  is asymptotically normal.
- (ii) if  $k < m$ ,  $\tilde{R}_j(k)$  is asymptotically right-skewed.

Intuitively, if all of the pervasive factors are removed in the residual, i.e.,  $k \geq m$ , then the factors in the residual can be thought of as an accumulated noise, and by Theorem 1, the residual length has a limiting normal distribution. On the other hand, if one or more pervasive factors remain in the residual, that is,  $k < m$ , then the sum of squared factors appears in the residual length. Condition 4 ensures that the squared factors are right-skewed.

### 3.3. The case of estimated principal component directions

When the estimated principal component directions  $\hat{u}_i$  are used, the residual lengths  $R_j(k)$  have different limiting distributions than those of  $\tilde{R}_j(k)$ . We characterize the full family of asymptotic distributions of  $R_j(k)$  under the null and alternative hypotheses. For this, we consider an asymptotic scenario where the limits  $d \rightarrow \infty$  and  $n \rightarrow \infty$  are taken progressively. This

resembles the case where the dimension increases at a much faster rate than the sample size does, such as  $d/n \rightarrow \infty$ , but is not identical to it (Lee et al., 2014). Asymptotic null distributions of  $R_j(k)$  for fixed  $n$  are discussed in the supplementary material.

Let  $\hat{w}_{ij} = \hat{u}_i^\top X_j$  denote the sample projection score. The following decomposition is useful in explaining the limiting distribution of  $R_j(k)$ :

$$R_j(k) = \tilde{R}_j(k) + a_j(k), \quad a_j(k) = \frac{1}{d} \sum_{i=1}^k (w_{ij}^2 - \hat{w}_{ij}^2). \quad (11)$$

First consider the asymptotic null distribution of  $R_j(k)$  under  $H_k : m = k$ . The over-estimated  $\lambda_i$  ( $i = 1, \dots, m$ ) by  $\hat{\lambda}_i$  leads that  $\hat{w}_{ij}^2$  tends to be larger than  $w_{ij}^2$  (shown in the supplementary material). Thus one can expect that  $a_j(m)$ , the difference between the squared true score and sample score, is negative. It turns out that  $a_j(m)$ , and subsequently  $R_j(m)$ , are in fact left-skewed in the limit, as shown in the following theorem. Describing the alternative distribution of  $R_j(k)$  for  $k < m$  seems a bit more challenging, at first glance. This is because the two dependent variables in (11) exhibit different skewness; the first term,  $\tilde{R}_j(k)$ , is asymptotically right-skewed, and the second term,  $a_j(k)$ , is asymptotically left-skewed. Below, we also show that  $a_j(k)$  is in fact asymptotically negligible.

**THEOREM 2.** *Assume the  $m$ -factor model under Conditions 1–4. Let  $m \geq 0$  be fixed. Suppose that the limits  $d \rightarrow \infty$  and  $n \rightarrow \infty$  are taken progressively.*

- (i) *(Global null) If  $m = 0$ , then in the limit, for each  $j$ ,  $R_j(0)$  is normally distributed, and for  $j \neq \ell$ ,  $R_j(0)$  and  $R_\ell(0)$  are independent.*
- (ii) *(Non-trivial null) If  $m \geq 1$ , then for each  $j$ ,  $n(R_j(m) - \tau^2) \rightarrow A_j(m)$  in probability, where  $A_j(m) = -\tau^2 \sum_{i=1}^m z_{ij}^2$ . Moreover, the random variables  $A_j(m)$  ( $j = 1, 2, \dots$ ) are identically distributed, left-skewed and independent with each other.*

(iii) (Alternative) If  $m > k \geq 0$ , then for each  $j$ ,  $R_j(k) \rightarrow B_j(k, m)$  in probability, where

$$B_j(k, m) = \sum_{i=k+1}^m \sigma_i^2 z_{ij}^2 + \tau^2. \text{ Moreover, the random variables } B_j(k, m) \text{ (} j = 1, 2, \dots \text{)}$$

are identically distributed, right-skewed and independent with each other.

Theorem 2 provides a theoretical justification for the test procedures based on the skewness in Section 2.2. The test statistics in (6)-(7) tend to be large under the non-trivial null hypothesis, and small under the alternative. Theorem 2 also implies that the sharp transition of p-values, from low to high, as shown in Fig. 1 is bound to happen for large enough  $d$  and  $n$ .

Our next result shows that our estimator (8) consistently estimates the true number of principal components. For this, we require the test involved be consistent and the function  $p_k$  be continuous for each  $n$ . These hold if  $p_k^D$  is used. Although  $p_k^R$  does not satisfy the continuity condition, the estimator of  $m$  using the triples test appears to be consistent in our empirical results.

**THEOREM 3.** *Assume the  $m$ -factor model under Conditions 1–4. Let  $\hat{m}(\alpha)$  be the estimator of  $m$  defined in (8), where  $p_k$  is computed using (7). Then for any  $\alpha \in (0, 1)$ ,*

$$\lim_{n \rightarrow \infty} \lim_{d \rightarrow \infty} \text{pr}(\hat{m}(\alpha) = m) = 1.$$

Theorem 3 not only shows a consistency but also suggests that for large enough dimension and sample size, the estimator  $\hat{m}$  should be nearly invariant to different choices of  $\alpha$ . This robustness against varying  $\alpha$  is empirically confirmed in Section 4.4.

## 4. NUMERICAL STUDIES

### 4.1. Existing methods to compare

There are a number of existing methods for determining the number of components. For  $d \ll n$  case, we refer to Jolliffe (2002) for an extensive list and discussion of heuristic and model-based methods.

Bai & Ng (2002) considered the problem of determining the number of principal components,  $m$ , when both the dimension and sample size diverge. There are several information-criteria type estimators proposed in their work, but we found directly using these estimators yield unsatisfactory results in our experiments. For our empirical studies, we use a modified estimator based on their information criteria, defined in the supplementary material. Simulation-based methods such as parallel analysis (Horn, 1965) have evolved into eigenvalue-based estimations of  $m$ , using an asymptotic random matrix theory for large  $d$  and  $n$ . Kritchman & Nadler (2008, 2009) and Passemier & Yao (2012, 2014) developed estimators of  $m$  using Tracy-Widom distribution (*cf.* Johnstone, 2001). Leek (2011) also proposed an eigenvalue-based estimator of  $m$  by choosing a stable threshold for the sample eigenvalues.

Our estimators obtained by (8) will be denoted by  $\hat{m}_R$  and  $\hat{m}_D$ , when using the p-value sequences of (6) and (7), respectively. For simplicity, we have used  $\alpha = 0.1$  for all numerical results. Our methods are in fact robust to different choices of  $\alpha$ , as further discussed in Section 4.4. In the numerical studies below, the performances of our estimators are compared with the methods of Kritchman & Nadler (2008), Passemier & Yao (2014), Leek (2011) and Bai & Ng (2002).

#### 4.2. Real data examples

We report the estimated number of components for eight real data sets. The first six are from gene expression studies, which usually produce high-dimensional data with limited sample size. The latter two data are two different types of images. These data sets are described in the following, and the result is summarized in Table 1.

The microarray data sets we tested include Diffuse large B-cell lymphoma data (*DLBCL*, Shipp et al., 2002), *Prostate* cancer data (Singh et al., 2002), and each of the two different platforms of the *NCI60* cell line data (Shoemaker, 2006). We also tested the training set of *Leukemia*

Table 1. *Number of principal components estimated from real data sets*

Type	Data set	$(d, n)$	$\hat{m}_R$	$\hat{m}_D$	$\hat{m}_L$	$\hat{m}_{KN}$	$\hat{m}_{PY}$	$\hat{m}_{BN}$
Gene	DLBCL	(7129, 77)	11	11	31	65	65	10
	Prostate	(2135, 102)	22	22	14	52	25	14
	NCI60 (cDNA)	(2267, 60)	5	5	2	31	9	2
	NCI60 (Affy)	(2267, 60)	10	10	23	44	31	4
	NCI60 (combined)	(2267, 120)	11	11	65	86	80	4
	Leukemia	(3051, 38)	1	9	9	25	22	3
	Lung	(2530, 56)	9	9	55	41	31	7
	Lobular Freeze	(16615, 817)	118	92	20	481	171	29
Image	Hippocampi	(336, 51)	11	11	14	27	24	3
	Liver	(12813, 500)	71	151	171	416	290	137

$\hat{m}_R$  our estimator using (6);  $\hat{m}_D$  our estimator using (7);  $\hat{m}_L$ , Leek (2011) method;  $\hat{m}_{KN}$ , Kritchman & Nadler (2008) method;  $\hat{m}_{PY}$ , Passemier & Yao (2014) method;  $\hat{m}_{BN}$ , Bai & Ng (2002) method.

data (Golub et al., 1999) and *Lung* cancer data (Bhattacharjee et al., 2001). The *Lobular Freeze* data set is a breast cancer gene expression data, measured by RNA sequencing (Ciriello et al., 2015).

The *hippocampi* data set (Pizer et al., 2013) consists of skeletal-representations, 3-dimensional models of human organs, parameterized by spatial locations, lengths and directions of skeletal spokes. Pizer et al. (2013) proposed a non-classical principal component analysis based on Jung et al. (2012a) to handle the complex data set. This data example is chosen to show that our method can be applied to a non-classical principal component analysis through scores matrix, since the residual lengths can be computed from the scores; see (11). The last data set consists of cell nucleus grayscale images from human *liver* tissues (Wang et al., 2011). we chose  $d = 12813$  variables with standard deviation greater than 0.01 from the original 36864 pixels.

The estimates in Table 1 show that our estimates  $\hat{m}_R$  and  $\hat{m}_D$  are similar to each other. There is a clear tendency that our estimates are generally larger than the estimates of Bai & Ng (2002), but smaller than the estimates of Kritchman & Nadler (2008) and Passemier & Yao (2014). Through a simulation study (summarized in Section 4.3), we have come to believe that the method of Bai & Ng tends to underestimate, while Kritchman & Nadler and Passemier & Yao overestimate, for finite  $d$  and  $n$ . In particular, the estimates  $\hat{m} = 25$  and  $22$  from the methods of Kritchman & Nadler and Passemier & Yao for the leukemia data seem unsuitably large considering the sample size  $n = 38$ . Our estimates, especially  $\hat{m}_D$ , exhibit a balance between two extremes. The seemingly biased other estimates are in part caused by the violation of distributional assumptions such as normality and equal tail-eigenvalues, which might be the case for real data sets. Our estimates do not need such assumptions.

#### 4.3. Simulation

To better understand the empirical performances of the estimators, we conducted a simulation study. The eigenvalues of  $\Sigma_d$  are modeled using  $s > 0$  representing a signal strength,  $0 \leq \beta < 1/2$  representing a decay rate of variances in noise components, and  $g > 0$  controlling the gap between leading eigenvalues, by

$$\lambda_i = \begin{cases} \sigma_i^2 d, & \sigma_i^2 = s^2 \{1 + g(m - i)\}, i = 1, \dots, m; \\ \tau_\beta i^{-\beta}, & m < i \leq d, \end{cases} \quad (12)$$

where  $\tau_\beta = \{\sum_{i=m+1}^d i^{-\beta} / (d - m)\}^{-1}$  is used to ensure that the average of  $\lambda_i$  ( $i = m + 1, \dots, d$ ) is 1. The eigenvectors of  $\Sigma_d$  are randomly chosen from the uniform distribution on the orthogonal group of dimension  $d$ .

We present simulation results for four different cases:

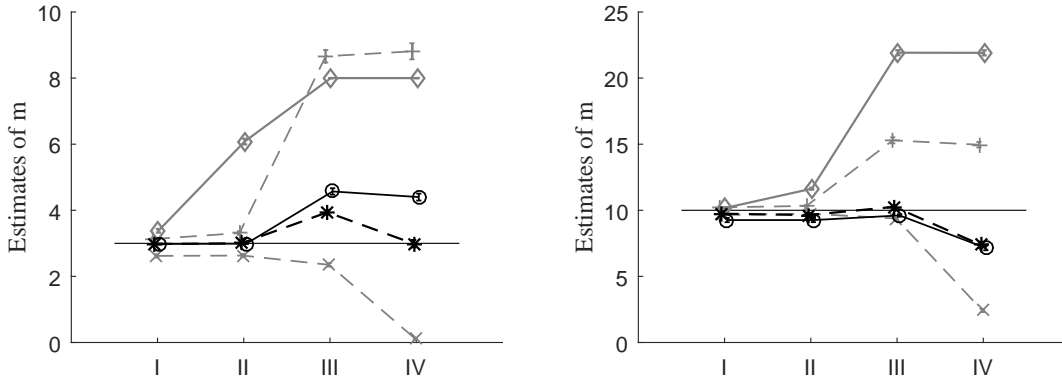


Fig. 2. Left:  $m = 3$  model. Averages and standard errors of estimates of the number of components;  $\hat{m}_R$  (circle-solid),  $\hat{m}_D$  (asterisk-dashed), Kritchman & Nadler (2008) estimator (gray plus-dashed), Passemier & Yao (2014) estimator (gray diamond-solid) and Bai & Ng (2002) estimator (gray x-dashed). The estimates of Leek (2011) were similar to Bai & Ng (2002), thus omitted. Right:  $m = 10$  model. The largest standard error for all results is 0.25.

- Case I: The standard normal distribution is used for sampling of the standardized scores  $z_{ij}$ . The eigenvalues of population covariance matrix is defined by (12) with  $(s, g, \beta) = (0.2, 1, 0)$ .
- Case II: The standard normal model with  $(s, g, \beta) = (0.2, 1, 0.3)$ .
- Case III: The  $t_3$  distribution model with  $(s, g, \beta) = (0.2, 1, 0.3)$ .
- Case IV: The  $t_3$  distribution model with  $(s, g, \beta) = (0.1, 0.5, 0.3)$ .

We set the true number of components  $m = 3, 10$  for each of the cases and collected the estimated results for  $(d, n) = (10000, 100)$  based on 100 simulation runs. The results in Fig. 2 show that our estimators  $\hat{m}_D$  and  $\hat{m}_R$  perform as well as or better than the competing estimators.

Case I is an ideal situation for all methods considered. In particular, the variances of noise components are equal to each other ( $\lambda_i = 1$ , for all  $i = m + 1, \dots, d$ ), and the normal assumption is satisfied. All methods perform similarly. In the settings with slowly-decreasing tail-eigenvalues (Case II), the methods of Kritchman & Nadler (2008) and Passemier & Yao (2014) tend to overestimate. This is because, for  $\beta > 0$ , the equal tail-eigenvalue assumption for the estimators of

Kritchman & Nadler and Passemier & Yao to be consistent is not satisfied. The assumptions for consistency of our estimators are satisfied under Case II.

In cases III and IV, a scaled  $t$  distribution with degrees of freedom 3 is used to sample the standardized scores  $z_{ij}$ . The coefficient of skewness in Condition 4 is not defined for this heavy-tailed distribution. Nevertheless, our estimators are less affected by the violation of the assumption compared to the more biased estimators of Kritchman & Nadler and Passemier & Yao. This is because the heavy-tailed scores exhibit more drastic distinctions of the left- and right-skewness than using the normal distribution. In Case IV, the leading  $m$  eigenvalues are smaller than in Case III. In this weak signal setting, both estimators of Leek (2011) and Bai & Ng (2002) are severely underestimating.

More simulation results, including larger  $d$ , larger  $m$ , various settings of  $(s, g, \beta)$ , and the conventional  $n > d$  case, are reported in the supplementary material.

#### 4.4. Empirical robustness against varying $\alpha$

The asymptotic invariance of  $\hat{m}$  against varying  $\alpha \in (0, 1)$ , shown in Theorem 3, suggests some degrees of invariance for moderately large  $d$  and  $n$ . In fact, for most real and simulated data examples we considered, the values of  $\hat{m}$  are stable against various values of threshold  $\alpha$ .

For a real data set of Shipp et al. (2002), introduced in Section 4.2, it is confirmed that our estimates  $\hat{m}_R(\alpha)$  and  $\hat{m}_D(\alpha)$  are stable for a wide range of  $\alpha$ ; see Fig. 3. As a comparison, we also have experimented on the eigenvalue-based estimators of Kritchman & Nadler (2008) and Passemier & Yao (2014) by changing their threshold value, which is parameterized by the  $1-\alpha$  quantiles of Tracy-Widom distribution. These estimates change their values more substantially. (The methods of Leek (2011) and Bai & Ng (2002) are not subject to arbitrary choices of threshold, thus excluded from this study.) We further compare to a heuristic method using the

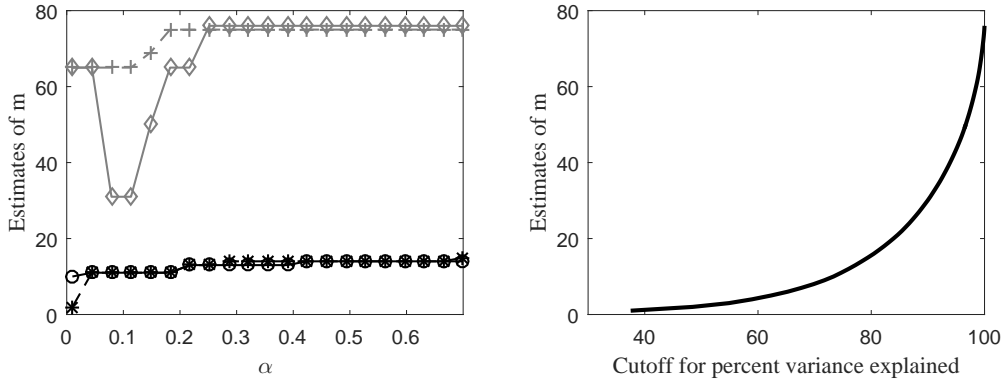


Fig. 3. Estimates  $\hat{m}$  as functions of  $\alpha$  (left panel) or as a function of the variance threshold (right panel), computed from a real data set of Shipp et al. (2002);  $\hat{m}_R$  (circle-solid),  $\hat{m}_D$  (asterisk-dashed), Kritchman & Nadler (2008) estimator (gray plus-dashed), Passemier & Yao (2014) estimator (gray diamond-solid).

cumulative percentage of variance explained. As shown in the right panel of Fig. 3, changing the threshold, say from 80% to 90%, would drastically change the estimates.

The robustness of our estimators against varying  $\alpha$  is also confirmed in simulated data. In Fig. 4, the estimates with varying  $\alpha$  are plotted for data generated by Case II in Section 4.3. Our estimates are stable, except for small values of  $\alpha < 0.1$ . The estimator of Kritchman & Nadler is also stable for larger values of  $\alpha$ , but the corresponding estimates are clearly biased.

## 5. PRINCIPAL COMPONENT SCORES IN HIGH DIMENSION

We conclude with a formal statement on the usefulness of the sample principal component scores in high dimensions.

Recall that  $W_1 = (\sigma_i z_{ij})_{i,j}$  is the  $m \times n$  matrix of the scaled true scores, and  $W_1 W_1^T$  is proportional to the  $m \times m$  sample covariance matrix of the first  $m$  scores. Similarly, we define  $\widehat{W}_1^T = d^{-1/2} \mathcal{X}(\hat{u}_1, \dots, \hat{u}_m)$ . Let  $\{\lambda_i(S), v_i(S)\}$  denote the  $i$ th largest eigenvalue-eigenvector pair of a non-negative definite matrix  $S$  and  $v_{ij}(S)$  denote the  $j$ th loading of the vector  $v_i(S)$ .

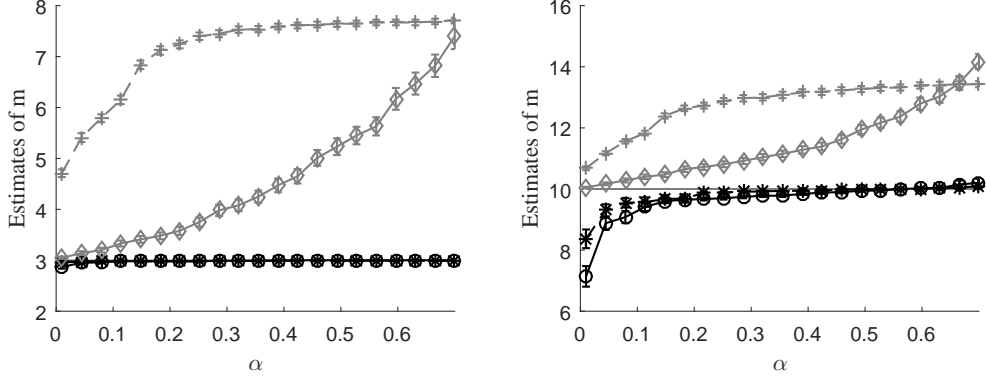


Fig. 4. Estimates as functions of  $\alpha$ , compared with the true values of  $m = 3$  (left) and 10 (right). Shown are the averages with standard errors from 100 simulation runs;  $\hat{m}_R$  (circle-solid),  $\hat{m}_D$  (asterisk-dashed), Kritchman & Nadler (2008) estimator (gray plus-dashed), Passemier & Yao (2014) estimator (gray diamond-solid)

**THEOREM 4.** *Assume the  $m$ -factor model under Conditions 1–4 and let  $n > m \geq 0$  be fixed.*

*In addition, we assume the scores  $w_{kj}$  are absolutely continuous.*

- (i) *If  $k \leq m$ , then the ratio of the sample score to the true score of  $X_j$  for the  $k$ th component is asymptotically decomposed into a common factor, not depending on  $j$ , and an error specific to each data point. Specifically,*

$$\frac{\hat{w}_{kj}}{w_{kj}} = \rho_k v_{kk} (W_1 W_1^T) + \varepsilon_{kj} + O_p(d^{-1/4}) \quad (j = 1, \dots, n),$$

where  $\rho_k = \{1 + \tau^2 / \lambda_k(W_1 W_1^T)\}^{1/2}$  and  $\varepsilon_{kj} = \rho_k \sum_{1 \leq i \leq m, i \neq k} \sigma_i z_{ij} (\sigma_k z_{kj})^{-1} v_{ki} (W_1 W_1^T)$ .

Moreover,

$$\widehat{W}_1^T = W_1^T R S + O_p(d^{-1/4}), \quad (13)$$

where  $R = [v_1(W_1 W_1^T), \dots, v_m(W_1 W_1^T)]$  is an  $m \times m$  orthogonal matrix, and  $S$  is the  $m \times m$  diagonal matrix whose  $k$ th diagonal element is  $\rho_k$ .

- (ii) *If  $k > m$ , then the ratio diverges with the rate  $d^{(1-\gamma_k)/2}$ , for  $\gamma_k$  satisfying  $\lambda_k \asymp d^{\gamma_k}$ . Specifically,  $\hat{w}_{kj}/w_{kj} = O_p(d^{(1-\gamma_k)/2})$  and  $d^{-1} \sum_{j=1}^n \hat{w}_{kj}^2 \rightarrow \tau^2$  in probability, as  $d \rightarrow \infty$ .*

The asymptotic relation (13) tells that for large  $d$ , the first  $m$  sample scores in  $\widehat{W}_1$  converges to the true scores in  $W_1$ , uniformly rotated and scaled for all data points. It is thus valid to use the first  $m$  sample principal scores for exploration of important data structure, to reduce the dimension of the data space from  $d$  to  $m$  in the high dimension, low sample size context.

#### ACKNOWLEDGEMENT

The authors are very grateful to the editor, associate editor and anonymous referees for their careful reading and thoughtful suggestions.

#### SUPPLEMENTARY MATERIAL

Supplementary material available at *Biometrika* online includes technical details and additional data examples.

#### REFERENCES

- AHN, J., MARRON, J. S., MULLER, K. M. & CHI, Y.-Y. (2007). The high-dimension, low-sample-size geometric representation holds under mild conditions. *Biometrika* **94**, 760–766.
- BAI, J. & NG, S. (2002). Determining the number of factors in approximate factor models. *Econometrica* **70**, 191–221.
- BAIK, J. & SILVERSTEIN, J. W. (2006). Eigenvalues of large sample covariance matrices of spiked population models. *J. Multivar. Anal.* **97**, 1382–1408.
- BHATTACHARJEE, A., RICHARDS, W. G., STAUNTON, J., LI, C., MONTI, S., VASA, P., LADD, C., BEHESHTI, J., BUENO, R., GILLETTE, M., LODA, M., WEBER, G., MARK, E. J., LANDER, E. S., WONG, W., JOHNSON, B. E., GOLUB, T. R., SUGARBAKER, D. J. & MEYERSON, M. (2001). Classification of human lung carcinomas by mRNA expression profiling reveals distinct adenocarcinoma subclasses. *Proc. Natl. Acad. Sci. USA* **98(24)**:137.
- CIRIELLO, G., GATZA, M. L., BECK, A. H., WILKERSON, M. D., RHIE, S. K., PASTORE, A., ZHANG, H., MCELLELLAN, M., YAU, C., KANDOTH, C. et al. (2015). Comprehensive molecular portraits of invasive lobular breast cancer. *Cell* **163**, 506–519.

- D'AGOSTINO, R. B. (1970). Transformation to normality of the null distribution of  $g_1$ . *Biometrika*, 679–681.
- D'AGOSTINO, R. B. & PEARSON, E. S. (1973). Tests for departure from normality. empirical results for the distributions of  $b_2$  and  $b_1$ . *Biometrika* **60**, 613–622.
- FAN, J., LIAO, Y. & MINCHEVA, M. (2013). Large covariance estimation by thresholding principal orthogonal complements. *J. R. Stat. Soc. B* **75**, 603–680.
- FARRELL, P. J. & ROGERS-STEWART, K. (2006). Comprehensive study of tests for normality and symmetry: extending the spiegelhalter test. *J. Stat. Comput. Simul.* **76**, 803–816.
- GOLUB, T. R., SLONIM, D. K., TAMAYO, P., HUARD, C., GAASENBEEK, M., MESIROV, J. P., COLLIER, H., LOH, M. L., DOWNING, J. R., CALIGIURI, M. A., BLOOMFIELD, C. D. & LANDER, E. S. (1999). Molecular classification of cancer: class discovery and class prediction by gene expression monitoring. *Science* **286**, 531–537.
- HALL, P., MARRON, J. S. & NEEMAN, A. (2005). Geometric representation of high dimension, low sample size data. *J. R. Stat. Soc. B* **67**, 427–444.
- HELLTON, K. H. & THORESEN, M. (2017). When and why are principal component scores a good tool for visualizing high-dimensional data? *Scand. J. Stat.*, to appear.
- HOLLANDER, M., WOLFE, D. A. & CHICKEN, E. (2013). *Nonparametric statistical methods*, vol. 751. John Wiley & Sons.
- HORN, J. L. (1965). A rationale and test for the number of factors in factor analysis. *Psychometrika* **30**, 179–185.
- JOHNSTONE, I. M. (2001). On the distribution of the largest eigenvalue in principal components analysis. *Ann. Stat.*, 295–327.
- JOLLIFFE, I. T. (2002). *Principal Component Analysis*. Springer Series in Statistics. New York: Springer-Verlag, 2nd ed.
- JOSSE, J. & HUSSON, F. (2012). Selecting the number of components in principal component analysis using cross-validation approximations. *Comput. Stat. Data Anal.* **56**, 1869–1879.
- JUNG, S., DRYDEN, I. L. & MARRON, J. S. (2012a). Analysis of Principal Nested Spheres. *Biometrika* **99**, 551–568.
- JUNG, S. & MARRON, J. S. (2009). PCA consistency in high dimension, low sample size context. *Ann. Stat.* **37**, 4104–4130.
- JUNG, S., SEN, A. & MARRON, J. (2012b). Boundary behavior in High Dimension, Low Sample Size asymptotics of PCA. *J. Multivar. Anal.* **109**, 190–203.
- KOLTCHINSKII, V., LOUNICI, K. et al. (2016). Asymptotics and concentration bounds for bilinear forms of spectral projectors of sample covariance **52**, 1976–2013.

- KOLTCHINSKII, V., LOUNICI, K. et al. (2017). Normal approximation and concentration of spectral projectors of sample covariance. *Ann. Stat.* **45**, 121–157.
- KRITCHMAN, S. & NADLER, B. (2008). Determining the number of components in a factor model from limited noisy data. *Chemometr. Intell. Lab.* **94**, 19–32.
- KRITCHMAN, S. & NADLER, B. (2009). Non-parametric detection of the number of signals: Hypothesis testing and random matrix theory. *IEEE Trans. Signal Process* **57**, 3930–3941.
- LEE, M. H. (2012). On the border of extreme and mild spiked models in the HDLSS framework. *J. Multivar. Anal.* **107**, 162–168.
- LEE, S., ZOU, F. & WRIGHT, F. A. (2014). Convergence of sample eigenvalues, eigenvectors, and principal component scores for ultra-high dimensional data. *Biometrika* **101**, 484.
- LEEK, J. T. (2011). Asymptotic conditional singular value decomposition for high-dimensional genomic data. *Biometrics* **67**, 344–352.
- PASSEMIER, D. & YAO, J. (2014). Estimation of the number of spikes, possibly equal, in the high-dimensional case. *J. Multivar. Anal.* **127**, 173–183.
- PASSEMIER, D. & YAO, J.-F. (2012). On determining the number of spikes in a high-dimensional spiked population model. *Random Matrices: Theory and Applications* **1**, 1150002.
- PAUL, D. (2007). Asymptotics of sample eigenstructure for a large dimensional spiked covariance model. *Stat. Sin.* **17**, 1617–1642.
- PIZER, S. M., JUNG, S., GOSWAMI, D., ZHAO, X., CHAUDHURI, R., DAMON, J. N., HUCKEMANN, S. & MARRON, J. S. (2013). Nested Sphere Statistics of Skeletal Models. In *Innovations for Shape Analysis: Models and Algorithms*, M. Breuß, A. Bruckstein & P. Maragos, eds., Lecture Notes in Computer Science. Springer.
- RANDLES, R. H., FLIGNER, M. A., POLICELLO, G. E. & WOLFE, D. A. (1980). An asymptotically distribution-free test for symmetry versus asymmetry. *J. Am. Stat. Assoc.* **75**, 168–172.
- SHIPP, M. A., ROSS, K. N., TAMAYO, P., WENG, A. P., KUTOK, J. L., AGUIAR, R. C., GAASENBEEK, M., ANGELO, M., REICH, M., PINKUS, G. S. et al. (2002). Diffuse large b-cell lymphoma outcome prediction by gene-expression profiling and supervised machine learning. *Nat. Med.* **8**, 68–74.
- SHOEMAKER, R. H. (2006). The NCI60 human tumour cell line anticancer drug screen. *Nat. Rev. Cancer* **6**, 813–823.
- SINGH, D., FEBBO, P. G., ROSS, K., JACKSON, D. G., MANOLA, J., LADD, C., TAMAYO, P., RENSHAW, A. A., D’AMICO, A. V., RICHIE, J. P. et al. (2002). Gene expression correlates of clinical prostate cancer behavior. *Cancer cell* **1**, 203–209.

WANG, W., OZOLEK, J. A., SLEPČEV, D., LEE, A. B., CHEN, C. & ROHDE, G. K. (2011). An optimal transportation approach for nuclear structure-based pathology. *IEEE Trans. Med. Imag.* **30**, 621–631.